

Climatology of the Eastern Arabian Sea during the last glacial cycle reconstructed from paired measurement of foraminiferal $\delta^{18}\text{O}$ and Mg/Ca

V. K. Banakar^{1*}, B. S. Mahesh¹, G. Burr², A. R. Chodankar^{1,3}

1. National Institute of Oceanography (CSIR), Dona Paula, Goa-403 004, India.

2. NSF-Arizona AMS Facility, 1118 E, 4th Street, Tucson, AZ85721-0081, USA.

3. Present address: B-6, Datta Apartments, Porvorim, Goa-403 008, India.

* - Corresponding author:

e-mail: banakar@nio.org; Ph: ++91-832-245-0361; Fax: ++91-832-245-0609

Abstract

Paired measurements of Mg/Ca and $\delta^{18}\text{O}$ of *Globigerinoides sacculifer* from an Eastern Arabian Sea (EAS) sediment core indicate that sea-surface temperature (SST) varied within 2°C and sea-surface salinity within 2 psu during the last 100 ka. SST was coldest (~27°C) during Marine Isotope Stage (MIS) 4 and 2. Sea-surface salinity was highest (~37.5 psu) during most of the last glacial period (~60 - 18 ka), concurrent with increased $\delta^{18}\text{O}_{G.sacculifer}$ and C/N ratios of organic matter and indicative of sustained intense winter monsoons. SST time series are influenced by both Greenland and Antarctic climates. However, the sea-surface salinity time series and the deglacial warming in the SST record (beginning at ~18 ka) compare well with the LR04 benthic $\delta^{18}\text{O}$ -stack and Antarctic temperatures. This suggests a teleconnection between the climate in the Southern Hemisphere and the EAS. Therefore, the last 100-ka variability in EAS climatology appears to have evolved in response to a combination of global climatic forcings and regional monsoons. The most intense summer monsoons within the Holocene occurred at ~8 ka and are marked by SST cooling of ~1°C, sea-surface salinity decrease of 0.5 psu, and $\delta^{18}\text{O}_{G.sacculifer}$ decrease of 0.2 ‰.

Key Words: Palaeoclimate, Arabian Sea, Mg-Ca SST, Surface salinity, Oxygen isotopes, Monsoons

MS statistics: Pages (Text + Figures) = 23; Words (Text + Figure Caption) = 4953; Figures = 5

Introduction

The glacial–interglacial variability and Dansgaard-Oeschger (D-O) oscillations observed in the Indian monsoon proxy records (Duplessy, 1982; Clemens et al., 1990; Anderson and Prell., 1993; Schulz et al., 1998; Reichert et al., 2002; Hong et al., 2003; Banakar et al., 2005; Chodankar et al., 2005, and references therein) demonstrate teleconnection between high latitude climates and Indian monsoons. The intensified southwest monsoons were found to coincide with shifts in surface temperature regimes of the Atlantic and Europe and the extent of ice sheets in northern hemisphere, not only during the Holocene (Overpeck et al., 1996) but also apparently continuing into modern times (see Goes et al., 2005).

These studies indicate the existence of complex teleconnections and possibly feedbacks between Indian monsoons and global climate (Krishnakumar et al., 1999), which are yet to be clearly understood. Therefore, the past variation in the Indian monsoon needs further study incorporating paired multi-proxy investigations and comparative assessment in the context of the global climate system. Time-series records of surface hydrographic and biogeochemical variability in the Arabian Sea provide valuable insights into past monsoon variability.

In this study we present paired measurements of oxygen isotopes and Mg/Ca-SST and estimated the residual $\delta^{18}\text{O}_{\text{SEAWATER}}$ (representing local salinity) for the EAS from SK117/GC8 sediment core. These climatological time series are further compared with previously published past global climate records and local productivity patterns to understand processes involved in driving the local climatology.

Mg/Ca ratios in planktonic calcite have been shown to preserve the ambient water temperature with considerable fidelity (Lea et al., 1999; Elderfield and Ganssen, 2000; Rosenthal et al., 2000; Dekens et al., 2001; Eggins et al., 2002; Sagawa et al., 2006), and salinity can be calculated using seawater $\delta^{18}\text{O}$ (Rostek et al., 1993; Delaygue et al., 2001; Dahl and Oppo, 2006). However, Rohling (2000) has demonstrated that the level of confidence in palaeo-salinity estimation from seawater $\delta^{18}\text{O}$ is poor, and hence we emphasize residual $\delta^{18}\text{O}_{\text{SEAWATER}}$ as opposed to absolute salinity to signify local change, unless otherwise warranted.

Material and methods

A 410-cm-long gravity core (SK117-GC8) was retrieved on board the *ORV Sagar Kanya* from the EAS (off Goa, India: 15°29'N; 72°51'E) at a water depth of 2500 m (Figure 1) for the present study. The AMS ^{14}C dating for the core-top section was obtained from the Van der Graaf Laboratory (Utrecht University, The Netherlands), and additional seven depth sections from the

upper 150-cm sections were dated at the NSF-AMS facility of the Arizona University (USA). The AMS ^{14}C dates were corrected for the local reservoir age of 500 yr (<http://intcal.qub.ac.uk>) before converting to calendar age using the CalPal-2005 program (Weninger et al., 2005). For radiocarbon dating, ~10 mg of calcite was obtained by mixing two planktonic foraminifer species (*G. ruber* and *G. sacculifer*) of 100-350 μm sizes.

The core-top section (0-2 cm) yielded an age of 2259 ± 64 cal yr BP. The *G. sacculifer* oxygen isotopes, organic carbon and C/N records for the present sediment core are from Banakar et al. (2005). The *G. sacculifer* oxygen-isotope depth series is tuned with eight radiocarbon dates, LR04 Benthic Oxygen Isotope Stack (Lisiecki and Raymo, 2005) and Youngest Toba Tuff (YTT: 71 ka) (Zeilinski et al., 1996) (Figure 2) to establish an improved time scale over the previously published SPECMAP-based relative chronology (Banakar et al., 2005; Chodankar et al., 2005).

The Mg/Ca measurements were made using the same species (*G. sacculifer* without terminal sac), size range (250-350 μm), and sediment depth intervals documented previously for the oxygen isotopes (Banakar et al., 2005; Chodankar, 2005). The *G. sacculifer* is relatively more resistant to dissolution as compared to other planktonic foraminifera (Delaney et al., 1985; Dekens et al., 2001) and has nearly uniform distribution of Mg between multiple chambers (Eggins et al., 2003), and hence is well suited for Mg/Ca-based SST reconstruction.

Around fifty visibly clean tests were picked under microscope and subjected to cleaning following the protocol of Elderfield and Ganssen (2000) as later refined by Barker et al. (2003). The tests were first gently crushed between two glass plates to break open all chambers and homogenized in a drop of water. Only the cleanest fragments were isolated from clay lumps, Mn-coated fragments, stained fragments and mineral grains using a fine brush. As this step greatly reduces the chance of oxide contamination, no separate Mn-reduction step was incorporated. The calcite fragments were repeatedly washed with ultrapure water followed by methanol to remove clays. The organic coatings were removed by treating the clay-free fragments in buffered H_2O_2 in a boiling water bath. To remove any secondary calcite deposition on the skeletons, the Mg-polishing was done by treating the clay and coating free fragments with 0.001 N HNO_3 . Every step in the cleaning protocol was followed by 30-60 seconds of sonication. Before the final dissolution in 1 ml of suprapure 0.75 M HNO_3 , the cleaned fragments were examined under the microscope to ensure only pristine calcite was taken for dissolution. The solutions were analyzed at the National Institute of Oceanography, India, on a Perkin-Elmer Optima 2000 DV ICP-OES calibrated with five multi-element calibration standards.

The Mg/Ca (mmol/mol) was obtained following intensity-ratio calibration (DeVilliers et al., 2002). A quality control (QC) solution with Mg/Ca of 2.75 mmol/mol was prepared in 0.75 M HNO₃ and analyzed after every fifth sample. The long-term average of QC (n = 72) measured over a period of one month during the analytical period was 2.72 ± 0.06 mmol/mol, yielding a precision of $\pm 0.6^\circ\text{C}$ for estimated SSTs. The Fe/Ca, Al/Ca and Mn/Ca (mmol/mol) were used for monitoring contamination. The scatter plots of the above ratios vs Mg/Ca (mmol/mol) yielded insignificant correlations ($R^2 = 0.09, 0.24$ and 0.02 respectively) suggesting that the measured Mg/Ca ratios were not influenced by contaminants.

The Mg/Ca ratios were translated in to SST following Dekens et al. (2002) *G. sacculifer*_{PACIFIC} calibration ($\text{Mg/Ca} = 0.37 \exp 0.09 [T - 0.36 (\text{Core Depth in km}) - 2^\circ \text{C}]$). We have assumed that the Mg/Ca–SST calibration for the same species as found in the tropical Pacific is appropriate for EAS, because these two regions are connected within the El Niño–Southern Oscillation (ENSO) monsoon system and experience more or less similar ocean–atmosphere coupled processes (Webster and Fasullo, 2002). The standard errors on SST estimates associated with this calibration are 1.4 C. The sea-surface salinity was calculated using a salinity– $\delta^{18}\text{O}_{\text{SEAWATER}}$ relationship from the Arabian Sea (Dahl and Oppo, 2006). For this, the local seawater $\delta^{18}\text{O}$ was obtained using the equation of Epstein et al (1953) after correcting the $\delta^{18}\text{O}_{G.sacculifer}$ for the global ice effect (Shackleton, 2000). Thus, the $\delta^{18}\text{O}_{\text{SEAWATER}}$ reflects the local surface salinity (henceforth, ‘salinity’) in the EAS. The standard errors in salinity estimation are 0.2 psu, hence we do not discuss salinity changes <0.4 psu. Although we are aware of the limitations in salinity estimation from local $\delta^{18}\text{O}_{\text{SEAWATER}}$ (Rohling, 2000), an approximate quantification of past variation of salinity may be useful to understand the responses of EAS climatology to global and local forcing. The procedures followed for oxygen-isotope, organic-carbon and organic-nitrogen measurements are standard and available elsewhere (Banakar et al., 2005; Chodankar et al., 2005).

Results and discussion

The Mg/Ca ratios vary between 2.8 and 4.2 mmol/mol, which is in the expected range of planktic Mg/Ca ranges for tropical oceans (Lea et al., 2000; Barker et al., 2005; Dahl and Oppo, 2006; Saraswat et al., 2005, and references therein). The SST obtained from the core-top (29.1°C : Figure 3) is comparable to the modern SST ($\sim 28.5^\circ\text{C}$) at the core location (www.nodc.noaa.gov), and also to the Uk₃₇ SSTs of Holocene sections in a set of sediment cores from the EAS ($\sim 28.5^\circ\text{C}$: Sonzogni et al., 1998: see Figure 1).

The Glacial Termination-1 marking the beginning of the Holocene occurred at 13 cal ka BP and the commencement of the last glacial maximum (LGM = MIS2) is recorded at 29 cal ka BP (Figure 3). The former event shows a delay of 1 ka, while the latter shows an excellent agreement with oxygen isotope boundaries defined by the LR04 benthic stack (see Lisiecki and Raymo 2005). As per the oxygen isotope time series on a calendar-year time scale, the deglaciation began ~18 cal ka BP and the Holocene optimum reached at ~9 cal ka BP. The coldest period of the LGM marked by heaviest $\delta^{18}\text{O}$ (0.3 ± 0.1 ‰) spans a time interval between 27 and 18 cal ka BP (Figure 3). The LGM–Holocene shift in $\delta^{18}\text{O}_{G.sacculifer}$ after correcting for global ice volume is ~0.8 ‰, which could be accounted for glacial–interglacial change in SST and salinity due to monsoon variability. This change is consistent with several other published oxygen-isotope records for the Arabian Sea. The climate events identified in the present sediment core could be considered as typical for the EAS because, the structure of $\delta^{18}\text{O}_{G.sacculifer}$ record is highly consistent with the robust LR04 benthic stack (Lisiecki and Raymo, 2005) (Figure 3), and timings of the climate events are based on radiocarbon ages.

Eastern Arabian Sea-surface hydrographic variability and global climate

The overall SST variation for the last ~100 ka is within 2°C, which is comparable to the glacial cooling of <2.5°C extracted from several Arabian Sea sedimentary records (see Figure 1 caption). The SST exhibits subdued glacial–interglacial variability relative to $\delta^{18}\text{O}$ (Figure 2 and 3). Although our time resolution is not adequate to define D-O fluctuations, the SST trends seen in Figure 3 appear to qualitatively incorporate mixed signals of both northern and southern polar climates as depicted in the Vostok Temperature record (Petit et al., 1999) and the Greenland ice sheet oxygen-isotope record (Dansgaard et al., 1993). The coldest SSTs during MIS 4 closely overlap the stadial trend between D-O interstadial events 17-19, and MIS 3's moderately warmer SSTs follow the broad pattern between interstadials 5-15. On the other hand, the MIS 4, MIS 2, and deglaciation data are consistent with the Vostok temperature record (Figure 3).

The ice-volume-corrected salinity (local surface salinity) approximately follows the trend observed in the Antarctic temperature record and LR04 benthic $\delta^{18}\text{O}$ stack (Figure 3) and is consistently higher during the last glacial period (~60-18 ka BP). The EAS salinity depends largely on inflow of low salinity water from the Bay of Bengal (BoB) through winter-spring poleward coastal currents (Shetye et al., 1991; Shankar et al., 2002). The reasons for higher salinity in the EAS during the last glacial period might indicate weakened coastal currents as a result of either intensified winter monsoons (Chodankar et al., 2005), or weakened summer monsoons. The net effect is

increased salinity in the bay and reduced sea level difference between the BoB and EAS, namely a reduction in pressure gradient that drives the winter–spring coastal currents, which are largely responsible for freshening the EAS surface (Shetye et al., 1991; Shankar et al., 2002). Therefore, consistently higher salinity in the EAS during the last glacial period suggests influence of global climate on the local circulation.

In light of above observations, we interpret the past variability of EAS climatology as response to processes reflecting global climate and monsoon intensity. The faint impressions of Antarctic warming as stages of strong summer monsoons, in addition to clear reflection of D-O fluctuations in the Arabian Sea sedimentary records and other oceanic regions, has suggested coupled north–south climate operating in low latitudes influenced by ENSO forcing (Sirocko et al., 1999). In addition, the transmission of subantarctic-mode water has been invoked to provide a thermal connection between Southern Hemisphere climate and the Western Indian Ocean (Kiefer et al., 2006). These previously reported observations, along with our present time series of SST and salinity, provide evidence for high-latitude climate influences on the late Quaternary climatological evolution of the EAS.

A tight connection between northern and southern high-latitude climate following a bipolar seesaw model has been documented in ice cores (EPICA Community Members, 2006). The Antarctic warming occurring within the rising phase of northern hemisphere high-latitude summer insolation (Kawamura et al., 2007) has further strengthened the north–south polar climate linkages. In our opinion, this linkage might be acting as two forcing end members for low-latitude climates, with relatively variable influence depending upon the relative separation of a region from the end-member locations. The superposition of effects of monsoons and associated circulation on the influence of global climate appears to have resulted in observed mixed and complex responses in the surface climatology of the EAS.

Eastern Arabian Sea surface hydrographic variability and monsoon climate

The summer monsoon intensity is mainly responsible for high productivity all over the Arabian Sea, due to associated intense upwelling in the western Arabian Sea and lateral advection of nutrient-rich upwelled water (Wyrski, 1973). On the other hand, intense winter mixing and deepening of the mixed layer in the northern region together increase the productivity during winter monsoons (Madhupratap et al., 1996). These observations are consistent with the coupled physical–biological modeling results for the Indian monsoon system, which demonstrated that intensified monsoons (summer or winter) may be expected to cause cooling of the sea surface and increase in productivity together in most parts of the Arabian Sea (Murtugudde et al., 2007).

Isolating the relative importance of past variability in summer and winter monsoons is not feasible from SST records. SST variability also incorporates the global climate effect along with monsoon-forced surface cooling. Hence, there is a need for another robust proxy, such as salinity, to isolate the relative dominance of summer and winter monsoons during a given climate stage.

It is well known that the Indian summer monsoons are extremely moist, while winter monsoons are extremely dry (Wyrтки, 1973). This contrasting moisture load results in distinct changes in salinity of the northern Indian Ocean during summer and winter monsoons (Webster and Fasullo, 2002). In addition, the BoB is relatively more sensitive to salinity changes as it receives enormous amount of freshwater from Ganges-Brahmaputra river discharge during the summer monsoon. We examine our multi-proxy data essentially in the light of the preceding observation.

The salinity time series shows variation up to 2 psu during the last 100 ka, and the largest gradient occurs between ~18 and ~9 cal ka BP (deglacial period) (Figure 4). During most of the last glacial cycle (MIS 4 through MIS 2) the EAS has witnessed salinity higher by over 1 psu than the present (~36 psu). This high-salinity feature could be expected only if there existed long-sustained intense winter monsoons and weakened summer monsoons. In addition, advection of low-salinity water from BoB into the EAS was reduced during the last glacial period due to intensified winters (Chodankar et al., 2005). These two regional processes appear to have resulted in long sustained higher salinity in the EAS during most of the last glacial period.

The intensification of winter monsoon can be confirmed by elevated C/N ratios of the sedimentary organic matter in the same sediment core spanning the last glacial cycle (Figure 4). The Redfield ratio of C/N for pure marine organic matter is ~6.6. The ratios above this are possible only when terrestrial plant biomass or organic matter from exposed shelf region during glacial lowered sea level having higher C/N ratios (up to 35) (Walsh et al., 1991) are added to the marine sedimentary reservoir.

The preferential fractionation of N during post-depositional diagenesis (Walsh et al., 1981) resulting in temporal variability of present C/N data may be ruled out because the X-Y scatter diagram for C and N in the present sediment core exhibits a tight linear correlation ($R^2 = 0.93$) (Figure 5). Therefore, the time series of C/N (Figure 4) is attributed to temporally varied mixing of marine and terrestrial organic matter in the EAS. The calculated proportion of terrestrial organic matter, considering mixing of two end-members with C/N 6.6 and 35, is around 10 % during the last glacial cycle and nearly absent during the Holocene and last warm period. The increased input of terrestrial organic matter during the cold climate is expected because glacial winter winds (land towards sea: see Figure 1) are likely to have been stronger than the interglacial winter winds. Distinctly higher salinity during the last glacial cycle associated with increased terrestrial organic

matter input and productivity in EAS (Banakar et al., 2005) together suggest that the basin has experienced significant reduction in freshwater flux due to weakened summer monsoons, but it has remained productive due to enhanced winter upwelling and nutrient supply from surrounding land caused by intense winter winds.

The deglacial warming in the Antarctic atmosphere, monotonic increase of SST, and decrease of salinity in EAS until the commencement of the Holocene (Figure 3) are consistent with the evolution of Indian summer monsoons, which began to strengthen with global climate warming following the LGM. Within the Holocene, the sea-surface cooling of $\sim 1^{\circ}\text{C}$ and freshening of ~ 0.5 psu along with ~ 0.2 ‰-lowered $\delta^{18}\text{O}_{G.sacculifer}$ (Figure 3) centered on 8 cal ka BP indicate the strongest summer monsoons of the Holocene. This ~ 8 cal ka BP event appears to be characteristic of the Holocene monsoon history of the Arabian Sea, as the event has also been reflected in previous high-resolution multiproxy studies (Overpeck et al., 1996; Dahl and Oppo, 2006).

Conclusions

Past variability of the SST and salinity in the Eastern Arabian Sea appear to have influenced by both global climate and local monsoons. On one hand, the time series of SST exhibits a pattern comparable to likely pattern emerging from a combination of southern and northern high latitude climates. On the other hand, the time series of salinity and C/N ratios exhibit glacial–interglacial variability.

Sea-surface warming by $\sim 2^{\circ}\text{C}$ and freshening by ~ 1 psu concurrently occurring during the deglaciation indicate rapid reorganization of regional monsoons with global climate transition from cold to warm. A synchronous decrease of sea-surface temperature, surface salinity, and $\delta^{18}\text{O}_{G.sacculifer}$ at ~ 8 cal ka BP indicate most intense summer monsoons with the onset of full Holocene conditions in the EAS.

Acknowledgements

Constructive reviews and valuable suggestions by two anonymous reviewers and the associate and senior editors were of great benefit. The Ministry of Earth Sciences provided ship time to collect the present sediment core and the National Institute of Oceanography provided all logistic support. K. van der Borg of Utrecht University and De-Martino Mitzi of Arizona University carried out AMS-measurements for radiocarbon ages. BSM and ARC thank CSIR for providing them fellowships during the time of the present study. (This is NIO Contribution No:.....).

References

- Anderson, D. M., Prell, W. L., 1993. A 300 ka record of upwelling off Oman during the late Quaternary: Evidence of the Asian southwest monsoon. *Paleoceanography* 8, 193-208.
- Banakar, V. K., Oba, T., Chodankar, A. R., Kuramoto, T., Yamamoto, M., Minagawa, M., 2005. Monsoon related changes in sea surface productivity and water column denitrification in the Eastern Arabian Sea during last glacial cycle. *Marine Geology* 219, 99-108.
- Barker, S., Greaves, M., Elderfield, H., 2003. A study of cleaning procedures used for foraminiferal Mg/Ca paleothermometry. *Geochemistry Geophysics Geosystems* 4, 8407.
- Chodankar, A. R., 2004. Late Pleistocene sedimentation history in the Eastern Arabian Sea: Climate-productivity-weathering linkages. Ph.D. Thesis, National Institute of Oceanography-Goa University, pp. 126.
- Chodankar, A. R., Banakar, V. K., Oba, T., 2005. Past 100 ky surface salinity gradient response in the Eastern Arabian Sea to the summer monsoon variation recorded by $\delta^{18}\text{O}$ of *G. sacculifer*. *Global Planetary Change* 47, 135-142.
- Clemens, S. C., Prell, W. L., 1990. Late Pleistocene variability of Arabian Sea summer monsoon winds and continental aridity: Eolian records from the lithogenic components of deep-sea sediments. *Paleoceanography* 5, 109-145.
- Dahl, K. A., Oppo, D. W., 2006. Sea surface pattern reconstructions in the Arabian Sea. *Paleoceanography* 21, PA1014, doi:10.1029/2005PA001162.
- Dansgaard, W., Johnsen, S. J., Clausen, H. B., Dahl-Jensen, D., Gundestrup, N. S., Hammer, C. U., Hvidberg, S., Steffensen, J. P., Sveinbjornsdottir, A. E., Jouzel, J., Bond, G., 1993. Evidence for general instability of past climate from a 250 ka ice-core record. *Nature* 364, 218-220.
- Delaney, M. L., Be, A. H. W., Boyle, E. A., 1985. Li, Sr, Mg, Na in foraminiferal calcite shells from laboratory culture, sediment traps and sediment cores. *Geochimica et Cosmochimica Acta* 49, 1327-1341.
- Delaygue, G., Bard, E., Rollion, C., Jouzel, J., Stevenard, M., Duplessy, J. C., Ganssen, G., 2001. Oxygen isotope/salinity relationship in the northern Indian Ocean. *Journal of Geophysical Research* C106, 4565-4574.
- Dekens, P. S., Lea, D. W., Pak, D. K., Spero, H. J., 2002. Core-top calibration of Mg/Ca in tropical foraminifera: refining paleo-temperature estimation. *Geochemistry Geophysics Geosystems* 3, doi: 10.1029/2001GC000200.
- DeVilliers, S., Greaves, M. J., Elderfield, H., 2002. An intensity ratio calibration method for the accurate determination of Mg/Ca and Sr/Ca of marine carbonates by ICP-AES. *Geochemistry Geophysics Geosystems* 3, doi: 10.1029/2001GC000169.
- Duplessy, J. C., 1982. Glacial-interglacial contrasts in the northern Indian Ocean. *Nature* 295, 494-498.
- Eggins, S., Deckker, P., Marshall, J., 2003. Mg/Ca variation in planktonic foraminifera tests: implication for reconstructing paleo-seawater temperature and habitat migration. *Earth and Planetary Science Letters* 212, 291-306.
- Elderfield, H., Ganssen, G., 2000. Past temperature and $\delta^{18}\text{O}$ of surface ocean water inferred from foraminiferal Mg/calc ratios. *Nature* 405, 442-445.
- EPICA Community Members, 2006. One to one coupling of glacial climate variability in Greenland and Antarctica. *Nature* 444, 195-198.

- Epstein, S., Buchsbaum, R., Lowenstam, A., Uray, H. C., 1953. Revised carbonate-water isotopic temperature scale. *Bulletin of Geological Society of America* 64, 1315-1325.
- Goes, J., Prasad, T. G., Helga, R. G., Fasullo, J. T., 2005. Warming of the Eurasian landmass is making Arabian Sea more productive. *Science* 308, 545-547.
- Hong, Y. T., Hong, B., Lin, Q. H., Zhu, Y. X., Shibata, Y., Hirota, M., Uchida, M., Leng, X. T., Jiang, H. B., Xu, H., Wang, H., Yi, L., 2003. Correlation between Indian Ocean summer monsoon and north Atlantic climate during the Holocene. *Earth and Planetary Science Letters* 211, 371-380.
- Imbrie, J., Hays, J.D., Martinson, D. G., McIntyre, A., Mix, A. C., Moorley, J. J., Pisias, N. G., Prell, W. L., Shackleton, N. J., 1984. The orbital theory of Pleistocene climate: support from a revised chronology. In: Berger, A. (Ed.), *Milankovitch and climate, Part-1*, Springer, NY, pp. 269-305.
- Kawamura, K., Parrenin, F., Lisiecki, L., Uemura, R., Vimeux, F., Severinghaus, J. F., Hutterli, M. A., Nakazawa, T., Aoki, S., Jouzel, J., Raymo, M. E., Matsumoto, K., Nakata, H., Motoyama, H., Fujita, S., Goto-Azuma, K., Fujii, Y., Watanabe, O., 2007. Northern hemisphere forcing of climate cycles in Antarctica over the past 360,000 years. *Nature* 448, 912-916.
- Kiefer, T., McCave, I. N., Elderfield, H., 2006. Antarctic control on tropical Indian Ocean sea surface temperature and hydrography. *Geophysical Research Letters* 33, L24612.
- Krishnakumar, K., Rajgopalan, B., Cane, M. A., 1999. On the weakening relationship between the Indian monsoon and ENSO. *Science* 284, 2156-2159.
- Lea, D. W., Mashiotta, T. A., Spero, H. J., 1999. Controls on magnesium and strontium up-take in planktonic foraminifera determined by living culturing. *Geochimica et Cosmochimica Acta* 63, 2369-2379.
- Lea, D. W., Pak, D. K., Spero, H. J., 2000. Climate impact of late Quaternary equatorial Pacific sea surface temperature variation. *Science* 289, 1719-1724.
- Lisiecki, L. E., Raymo, M. E., 2005. A Pliocene-Pleistocene stack of 57 globally distributed benthic $\delta^{18}O$ records. *Paleoceanography* 20, PA1003: doi:10.1029/2004PA001071.
- Madhupratap, M., Kumar, S. P., Bhattatri, M. A., Kumar, M. D., Raghukumar, S., Nair, K. C., Ramaiah, N., 1996. Mechanism of biological response to winter cooling in the northeastern Arabian Sea. *Nature* 384, 549-552.
- Murtugudde, R., Seager, R., Prasad, T., 2007. Arabian Sea response to monsoon variations. *Paleoceanography* 22, PA4217.
- Overpeck, J., Anderson, D., Trumbore, D., Prell, W., 1996. The southwest Indian Monsoon over the last 18000 years. *Climate Dynamics* 12, 213-225.
- Petit, J. R., Jouzel, J., Raynaud, D., Barkov, N. I., Barnola, J. M., Basile, I., Bender, M., Chappellaz, J., Davis, M., Delaygue, G., Delmotte, M., Kotlyakov, V. M., Legrand, M., Lipenkov, Y. V., Lorius, C., Pepin, L., Ritz, C., Saltzman, E., Steivenard, M., 1999. Climate and atmospheric history of the past 420,000 years from Vostok ice core. Antarctica. *Nature* 399, 429-436.
- Reichart, G. J., Nortier, J., Versteegh, G., Zachariasse, W. J., 2002. Periodic breakdown of Arabian Sea oxygen minimum zone caused by deep convective mixing. In: Clift, P. D. et al., (eds.), *The tectonic and climate evolution of the Arabian Sea region*, Geological Society of London, Special Publication 195, pp. 407-419.
- Rohling, E. J., 2000. Paleosalinity: confidence limits and future applications. *Marine Geology* 163, 1-11.

- Rosenthal, Y., Lohmann, G. P., Lohmann, K. C., Sherell, R. M., 2000. Incorporation and preservation of Mg in Globigerinoides sacculifer: Implication for reconstructing the temperature and $^{18}\text{O}/^{16}\text{O}$ of seawater. *Paleoceanography* 15, 135-145.
- Rostek, F., Ruhland, G., Bassinot, F. C., Muller, P. J., Labeyrie, L. D., Lancelot, Y., Bard, E., 1993. Reconstructing sea surface temperature and salinity using $\delta^{18}\text{O}$ and alkenone records. *Nature* 364, 319-321.
- Sagawa, T., Toyoda, K., Oba, T., 2006. Sea surface temperature record off central Japan since the last glacial maximum using planktonic foraminiferal Mg/Ca thermometry. *Journal of Quaternary Science* 21, 63-73.
- Saraswat, R., Nigam, R., Weldeab, S., Mackensen, A., Naidu, P. D., 2005. A first look at past sea surface temperatures in the equatorial Indian Ocean from Mg/Ca in foraminifera. *Geophysical Research Letters* 32, L24605, doi:10.1029/2005GL024039.
- Schulz, H., von Rad, U., Erlenkeuser, H., 1998. Correlation between Arabian Sea and Greenland climate oscillations of past 110000 years. *Nature* 393, 54-57.
- Sirocko, F., Luischner, D., Staubwasser, M., Maley, J., Heusser, L., 1999. High-frequency oscillations of the last 70000 years in the tropical/subtropical and polar climates. In: *Mechanism of global climate change at millennial time scale. Geophysical Monograph* 112, American Geophysical Union, pp. 113-126.
- Shackleton, N. J., 2000. The 100,000 year ice-age cycle identified and found to lag temperature, carbon dioxide and orbital eccentricity. *Science* 289, 1897-1902.
- Shankar, D., Vinayachandran, P., Unnikrishnan, A. S., 2002. The monsoon currents in the north Indian Ocean. *Progress in Oceanography* 52, 63-120.
- Shetye, S. R., Gouveia, A. D., Shenoi, S. S. C., Micheal, G. S., Sundar, D., Almeida, A. M., Santanam, K., 1991. The coastal currents off western India during the northeast monsoon. *Deep Sea Research* 38, 1517-1529.
- Slingo, J., 2002. Monsoons: Overview. In: *Encyclopedia of atmospheric Sciences*, v.3, Academic Press, pp. 1365-1370.
- Sonzogni, C., Bard, E., Rostek, F., 1998. Tropical sea surface temperatures during the last glacial period: a view based on alkenones in Indian Ocean sediment. *Quaternary Science Reviews* 17, 1185-1201.
- Webster, P. J., Fasullo, J., 2002. Monsoons-Dynamic theory, in: *Encyclopedia of atmospheric Sciences*, Academic Press, v. 3, pp. 1370-1385.
- www.nodc.noaa.gov/OC5/WOA05E: Levitus and Boyer's Annual salinity and temperature online maps.
- Weninger, B., Joris, O., Danzeglocke, U., 2005. Cologne radiocarbon calibration and palaeoclimate research package-online: www.calpal-online.de.
- Wyrtki, K., 1973. Physical oceanography of the Indian Ocean. In: Zeitzschel, B (Ed.), *Biology of the Indian Ocean*. Springer, pp. 18-36.
- Zielinski, G. A., Mayewski, P. A., Meeker, L. D., Whitlow, S., Twickler, M. S., 1996. Potential atmospheric impact of the mega-eruption 71000 y ago. *Geophysical Research Letters* 23, 837-840.

Figure Captions

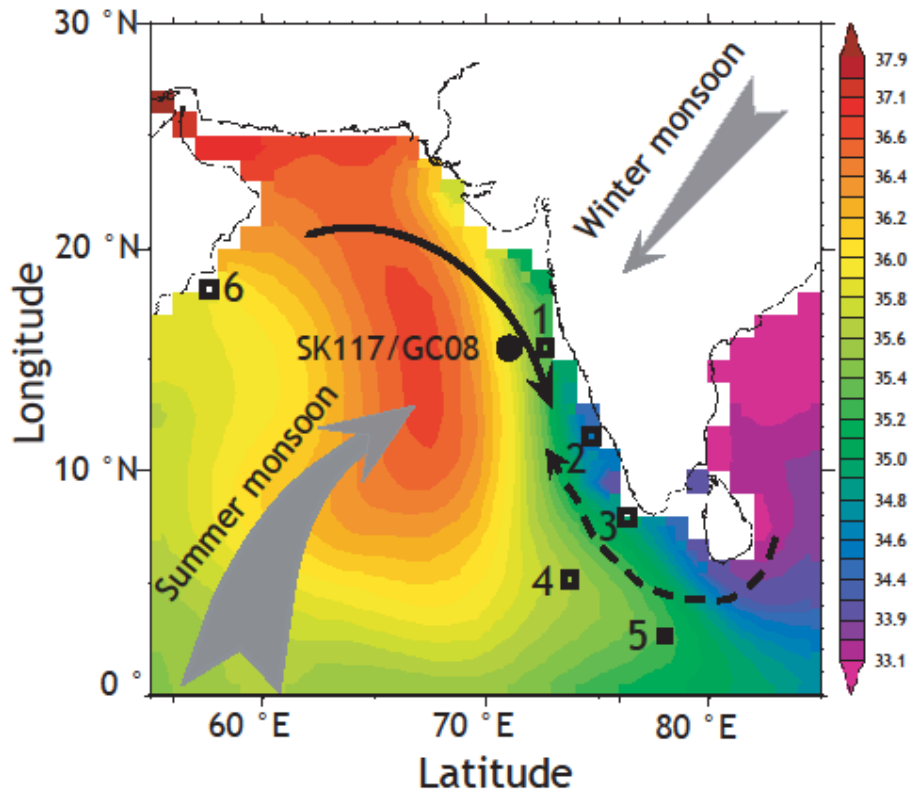
Figure 1. Location of SK117/GC8 sediment core (filled circle). The shaded block-arrows indicate modern reversing monsoon winds. Solid (broken) arrow indicates surface circulation during summer (winter) monsoons (Shankar et al., 2002). The numbered open boxes are the locations for which last glacial to Holocene SST gradient of $<2.5^{\circ}\text{C}$ was recorded (1-3 and 6, Uk₃₇ SST: Sonzogni et al., 1998; 4, Uk₃₇ SST: Rostek et al., 1993; 5, Mg-SST: Saraswat et al., 2005). The 175 ka SST record (4) from southeastern Arabian Sea does not exhibit clear glacial–interglacial or D-O patterns. Records 1-3 and 6 are only the last glacial and Holocene sections. The base map of annual surface salinity is adopted from www.noaa.nodc/WOA05.

Figure 2. Age model for SK117/GC8 based on a) eight radiocarbon dates (filled triangles: 1 cm = 2259 ± 64 cal yr BP; 15 cm = 8000 ± 37 cal yr BP; 25 cm = $12,887 \pm 100$ cal yr BP; 49 cm = $18,519 \pm 298$ cal yr BP; 79 cm = $25,214 \pm 393$ cal yr BP; 103 cm = $30,180 \pm 307$ cal yr BP; 125 cm = $33,905 \pm 433$ cal yr BP; 149 cm = $34,124 \pm 402$ cal yr BP), b) Marine Isotope Stage events (broken vertical lines labeled as MIS 3/4, 5.1, 5.2, 5.3) defined in LR04 benthic stack (Lisiecki and Raymo, 2005), and c) Youngest Toba Tuff (broken vertical line labeled as YTT) recorded in the Greenland ice cores at ~ 71 ka (Zeilinski et al., 1996).

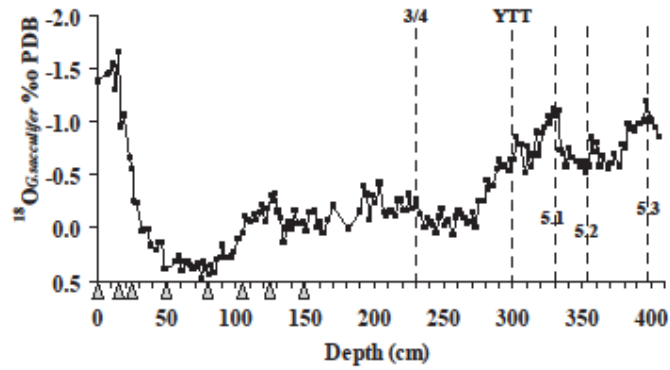
Figure 3. Composite time series (from bottom to top) of oxygen isotopes (SK117/GC8 and LR04 benthic stack); Residual (R) $\delta^{18}\text{O}_{\text{SEAWATER}}$ and estimated surface salinity; Mg/Ca ratios and estimated SST, and Antarctic temperatures (Petit et al., 1999) and Greenland ice-core oxygen isotopes (Dansgaard et al., 1993). Dotted vertical lines indicate marine isotope stage (bold numbered) boundaries and MIS5 peak interstadial and stadial events as recorded in LR04. The initiation of last deglaciation and YTT are shown with broken lines. The Greenland interstadials are labeled with small numbers. The *G. sacculifer* oxygen-isotope data for SK117/GC8 is from Banakar et al., (2005) and Chodankar et al., (2005). The coherency between residual $\delta^{18}\text{O}_{\text{SEAWATER}}$ and salinity, and Mg/Ca ratios and SST throughout the last 100 ka, indicate robustness of sedimentary proxies and calibrations used to extract past surface climatology of the EAS.

Figure 4. Time series of surface salinity and C/N ratios of organic matter in the studied sediment core. The horizontal broken line on the C/N-panel is the maximum expected Redfield Ratio (RR) for marine organic matter and upward arrow on the right-hand side denotes increasing contribution of terrestrial organic matter (TOM). The broken line on the salinity panel marks the modern surface salinity (MS) in the location of the sediment core (see Figure 1). C/N data are from Banakar et al. (2005).

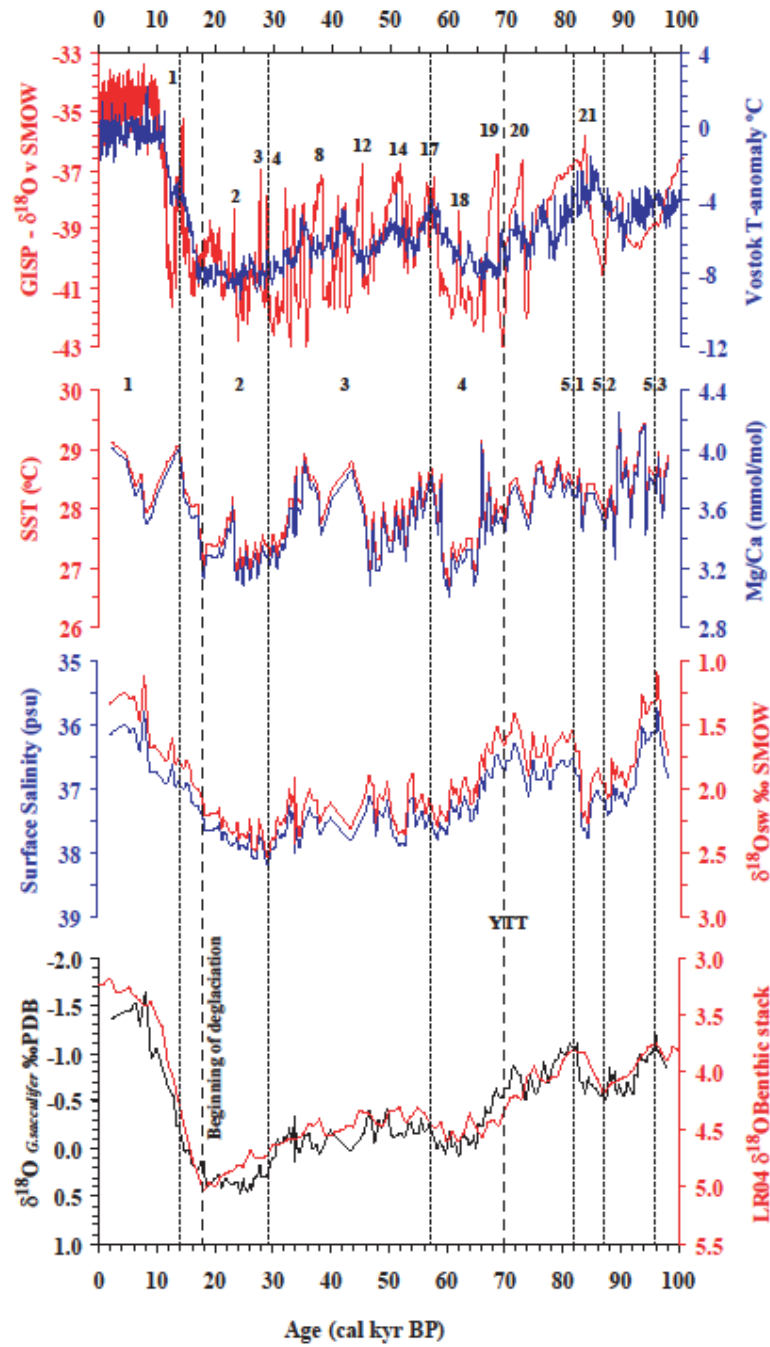
Figure 5. X-Y scatter plot of total organic carbon and organic nitrogen (data from Chodankar, 2004).

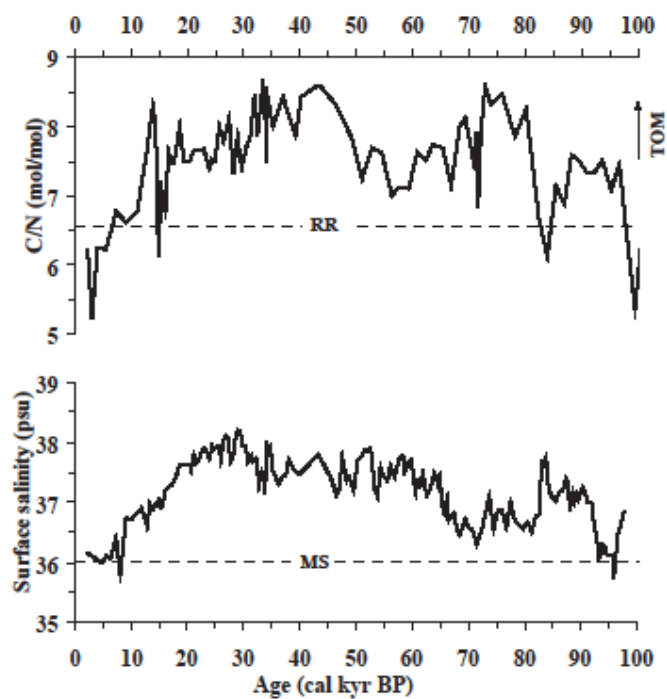


YQRES-D-09-0026: Banakar et al., Fig.2



YQRES-D-0026: Banakar et al., Fig.3





YQRES-D-09-0026: Banakar et al., Fig 5

